R-parity conserving SUSY studies with Jets and Missing Transverse Energy (E_T^{Miss})

1^{st} Year Transfer Report

Alexander Richards
Dept. Physics and Astronomy,
University College London

June 11, 2007

Abstract

This report sets out the work completed to date on detecting supersymmetric squark and gluino production over the standrd model backgrounds. The analysis so far, has concentrated largely on studying ways in which the supersmmetric signal may be discriminated from the large QCD jet background. It is shown that, by implementation of the cuts laid out within the report, the QCD background can be effectively reduced. Two other backgrounds, those from W→ eν & Z→ $\nu\bar{\nu}$ have also been considered to determine the efficacy of the cuts at reducing their contribution to the standard model background. This report also outlines the work completed for various other projects which have direct relevance to the main analysis before finally setting out the plans for future study.

Acknowledgements

With thanks to my supervisor Dr. Claire Gwenlan and Dr. Simon Dean for all their help and support throughout. In addition I wish to thank the STFC (formally PPARC) for financially supporting my Ph.D.

Contents

1 Introduction

1.1 The Standard Model and Beyond

The 'Standard Model' of particle physics represents our current best understanding of three of the four fundamental interactions of nature (electromagnetic, weak and strong) as well as a description of all experimental data. The model currently consists of 17 experimentally observed particles (12 fermions and 5 vector bosons). In addition to these the model postulates a new as yet undiscovered scalar boson called 'the Higgs' after Peter Higgs who first suggested it in an attempt to explain the electroweak symmetry breaking (1).

Although the standard model provides excellent agreement with experimental results, the model is by no means complete, one of its biggest shortcomings is the lack of a quantum field theory description of the fourth fundamental interaction in nature, gravity. In addition, the standard model treats neutrinos as massless objects; however, in 1998 Super-Kamiokande provided some evidence to the contrary by publishing results that indicated the existence of neutrino oscillations. The standard model also fails to explain the existence of dark matter in the universe, the strong CP problem and the universal matter-antimatter asymmetry.

1.2 Supersymmetry (SUSY)

Supersymmetry is the as yet unproven extension to the standard model which predicts a symmetry between fermions and bosons such that each standard model fermion has a scalar boson (spin 0) super partner and each standard model boson has a fermionic (spin 1/2) super partner, thereby at least doubling the number of particles in the model.

The main motivation for supersymmetry is as a solution to the so called hierarchy problem. Supersymmetry gets around this problem by having automatic cancellations between fermionic and bosonic Higgs interactions. An additional benefit of supersymmetry is that unlike with the standard model alone, it allows for the unification of the gauge couplings at some higher scale $\sim 10^{15}$ GeV. This is necessary for many grand unified theories (GUTs).

In supersymmetric extensions to the standard model, baryon number and lepton number are no longer conserved. This leads to such unfavourable physics as proton decay with a lifetime 10^{-2} seconds to 1 year, where the current observed proton lifetime is greater than $10^{33} - 10^{34}$ years (2). The solution is to impose R-parity on the model, defined as in equation 1, where standard model particles have R-parity of 1 whilst supersymmetric particles have R-parity of -1. In equation 1 j is the spin of the particle while B and L are the baryon and lepton quantum numbers respectively.

$$R = (-1)^{2j+3B+L} \tag{1}$$

Unlike lepton number or baryon number, the quantum number associated with R-parity is multiplicative not additive. This means that, in R-parity conserving models, SUSY particles must be pair produced and any SUSY particle interaction vertex must have two SUSY particles. For this reason, the lightest of the supersymmetric particles must be stable. This, along with the fact that supersymmetry is not an exact symmetry of nature, provides the supersymmetry model with a good dark matter candidate.

1.3 The LHC and ATLAS

The 'Large Hadron Collider' (LHC) is the next generation of high energy particle collider. Located at the 'European Centre for Nuclear Research' (CERN) in the old 'Large Electron Positron' (LEP) collider tunnel, it will collide 7 TeV protons head on at a centre of mass energy of 14 TeV. This previously unimaginably high collision energy will make the LHC both the largest and highest energy collider in the world.

The Collider, due to turn on for the first time within the next year has a design luminosity of $10^{34}\text{cm}^{-2}\text{s}^{-1}$. With the beams crossing every 25 ns, there will be 23 interactions per crossing at this luminosity (3).

Along its 27 km ring, the LHC has four interaction points at which are situated four different experiments. These are 'A Toroidal LHC ApparatuS' (ATLAS), the 'Compact Muon Solenoid' (CMS), 'A Large Ion Collider Experiment' (ALICE) and the 'Large Hadron Collider beauty experiment' (LHC-b). Both ATLAS and CMS are general purpose particle detectors, while the remaining experiments are more specialised. ALICE is a dedicated heavy ion detector, built to exploit the physics potential at the LHC. ALICE will be investigating a new state of matter known as the quark-gluon plasma (QGP). LHC-b will be investigating CP violation with B mesons.

ATLAS, like any general purpose detector, is constructed in layers with an 'onion-like' structure. Closest to the beam pipe there is the 'Inner Detector' (ID) which is responsible for measuring collision and decay vertices as well as tracking charged particles until they reach the calorimeters. The ID has a sub-structure consisting of three main parts, these are the pixel detector, the Semiconductor Tracker (SCT) and the Transition Radiation Tracker (TRT). The ID is surrounded by a solenoid magnet providing a field

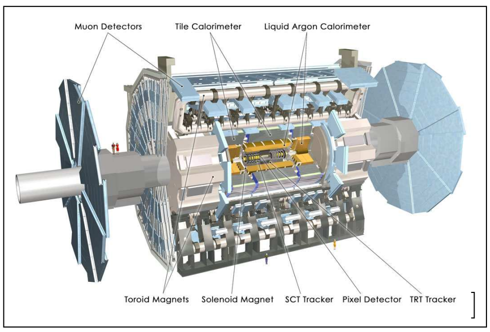

Figure 1: ATLAS Detector (4)

of 2T. This is of use in particle identification within the ID. Furthest away from the beam pipe are the muon detectors for detecting these most penetrating charged particles. These detectors have their own toroidal magnet system from which the experiment gets its name. Between the solenoid and the toroidal magnet systems are the calorimeters, firstly the electromagnetic and then the hadronic. The electromagnetic calorimeter is a sampling calorimeter with liquid Argon (LAr) scintillator and lead absorber. Of particular note for this report is the full coverage hadronic calorimeter provided by a large central barrel scintillator-tile cylinder and two smaller extended barrel cylinders. The combination of this excellent hadronic calorimeter coverage with a very granular good electromagnetic calorimeter means that ATLAS is well suited to the study of jets and missing transverse energy (E_T^{Miss}).

The positional co-ordinate system used in the ATLAS experiment is the (η,ϕ) co-ordinate system, where η is the so-called pseudo-rapidity which tends to the true rapidity for highly relativistic particles. The pseudo-rapidity is defined as is equation 2.

$$\eta = -\ln(\tan\frac{\theta}{2}) \tag{2}$$

Here θ is the regular polar angle as defined in the (x,y,z) co-ordinate system with the x axis pointing towards the centre of the LHC accelerator, the y axis vertically upwards, the z axis being parallel to the beam axis and being centred (as is the case with the detector itself) on the nominal p–p interaction vertex.

The pseudo-rapidity is defined in the range $-5 \leq \eta \leq 5$. It is also a physically desirable variable as differences in η are invariant under Lorentz boosts along the beam (z) axis.

2 Physics Studies

2.1 Jets and E_T^{Miss} Analysis

Jet production will be copious at ATLAS, it will be simple to observe and is also a good place to look for new physics (5). In this section an overview of the current state of the analysis to date will be presented as will all work completed for the AtlFast[1] and CSC3[2] groups.

The goal of the analysis is to investigate whether the production and subsequent decay of squarks and gluinos can be detected by looking for events with jets and large E_T^{Miss}. To this end, discriminating variables are investigated in order to determine whether they allow for the reduction of the large SM background. This report focuses mainly on QCD jets; however, W→ eν and Z→ $\nu\bar{\nu}$ are also considered with a mind for studying further backgrounds in the near future such as top ($t\bar{t}$) and Z→ ee. Having identified these variables, the next step would be to optimise them to give the best signal to background ratio.

2.1.1 Missing Transverse Energy E_T^{Miss}

E_T^{Miss} is a vector in the transverse plane to the beam axis (the x–y plane) which is equal in magnitude but opposite in direction to the net (of all particles in the event) energy-momentum vector in that plane. While the initial momentum of the beams in a hadron - hadron collider along the beam direction cannot be precisely known, it is true that the initial momentum perpendicular to the beam axis is zero. As a direct consequence of conservation of energy-momentum one expects that in the final state this should also be the case; therefore, a net energy-momentum vector in the transverse plane signifies among other things the loss of a particle from the detector owing to it not interacting (e.g. neutrinos etc.) and is referred to as missing transverse energy or E_T^{Miss}.

In QCD jet events the E_T^{Miss} can arise from neutrinos in the final state escaping the detector and is also from jet energy mis-measurements. In R-parity conserving SUSY events there is a large E_T^{Miss} arising from the existence of two (comparatively) 'light' stable neutralinos, the so called 'Lightest Supersymmetric Particles' (LSPs) in the final state. The jets in the Supersymmetry case come from the hadronic decays of the squarks. Owing to the heavy LSPs in the final state one expects SUSY events to have a relatively high E_T^{Miss}; whereas, one expects that the E_T^{Miss} in the QCD jet events, coming from jet energy mis-measurement and neutrinos (and not from the presence of two massive super particles), would be significantly lower.

The E_T^{Miss} therefore makes a good discriminatory variable between the 'standard model' and 'beyond the standard model' physics. Using the "official" ATLAS production 'pythia.jetjet.recon' J1-J8[3] and SUSY SU3[4] samples generated with software releases 11.0.42 and 11.0.5 respectively, the E_T^{Miss} distributions were plotted for both QCD jet and SUSY events. In this plot(Figure 2), 1000 QCD events were processed per J1-J8 sample compared to the 7000 SU3 SUSY events and both samples were analysed using the ATLAS offline software version 11.0.5. The plot was then normalised to a luminosity of $10fb^{-1}$. This led to a requirement being placed on the missing E_T of $E_T^{Miss} > 200$ GeV, which acts as a powerful QCD reducing cut.

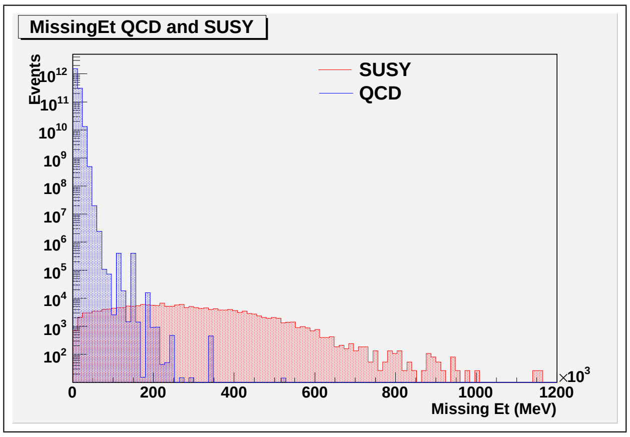

Figure 2: Missing Et Plot

2.1.2 The $\delta\phi$ Plots

Given its origins, one expects that in the QCD jet events the E_T^{Miss} should be reasonably co-linear with one or other of the jets' directions; whereas, in the squark production SUSY processes there is no such constraint. Another discriminating variable considered therefore was that of the relative direction of the E_T^{Miss} as compared to the jet direction of the two leading jets. This can be seen using the correlation in the $\delta\phi_1$ versus $\delta\phi_2$ plane (Figure 3).

Here the ATLAS offline software version 12.0.6 is used for the analysis, with the standard production 'pythia.jetjet.recon' J1-J8 jet samples for the QCD jet background and the production SU3 SUSY samples. Both of the data sets were produced in release 12.0.6, where $\delta\phi_1$ and $\delta\phi_2$ are defined as in equations 3 and 4.

$$\delta\phi_1 = |\phi_{j1} - \phi(E_T^{Miss})| \tag{3}$$
$$\delta\phi_2 = |\phi_{j2} - \phi(E_T^{Miss})| \tag{4}$$

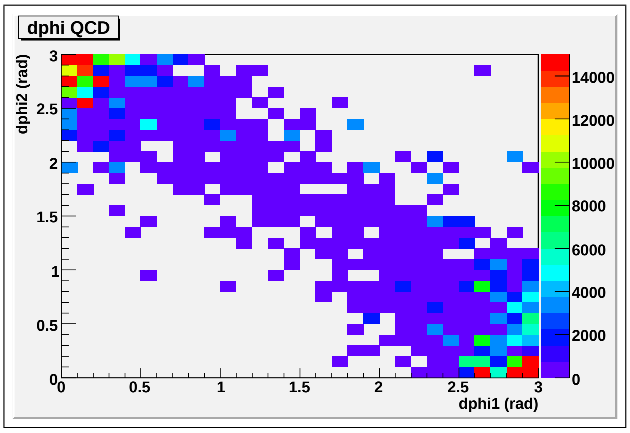

(a) QCD jet $\delta\phi$ plot

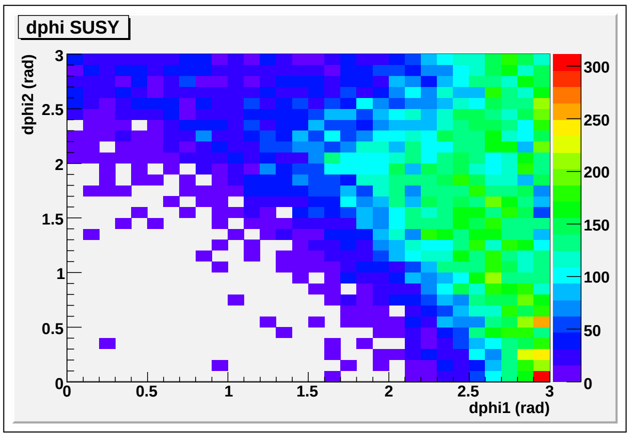

(b) SUSY $\delta\phi$ plot

Figure 3: $\delta\phi$ plots

In the QCD jet events, if the E_T^{Miss} is co-linear with one jet, the difference between it and the other jet will be approximately π (i.e. $\delta\phi_2 = \pi - \delta\phi_1$). It is therefore easy to see why the QCD $\delta\phi$ plot is as it is.

In order to improve the distinction between the QCD and SUSY in the above plots, it was necessary to implement some cuts on the jets. These 'jet cuts' included requiring that there be at least 3 jets in the event, with the hardest three having transverse energies of 180 GeV, 110 GeV and 100 GeV respectively. It was also required that the three hardest jets be within the range $|\eta| < 3$, with the hardest jet having $|\eta| < 1.7$. In addition, the E_T^{Miss} requirement of $E_T^{Miss} > 200$ GeV was used initially but due to its excellent discriminating power was later relaxed to $E_T^{Miss} > 45$ GeV in order that the above plots convey the difference in shape in the $\delta\phi_1$–$\delta\phi_2$ plane between QCD jet and SUSY events. In the analysis that led to the above plots, 10000 events were processed per J1-J8 sample and then they were weighted and normalised for a luminosity of $10fb^{-1}$. For the SU3 SUSY sample, 40000 events were processed and normalised to the same luminosity.

The highest E_T jets are usually the most accurately measured, so in the cases where the jet E_T is mis-measured the E_T^{Miss} is pulled closer in ϕ to the mis-measured jet(5). This can be clearly seen by plotting $\delta\phi_2$ for the QCD jets (Figure 4(a)). By doing so one observes a significantly higher peak at 0° in $\delta\phi_2$, representing the E_T^{Miss} lying along the direction of the second hardest jet the vast majority of the time.

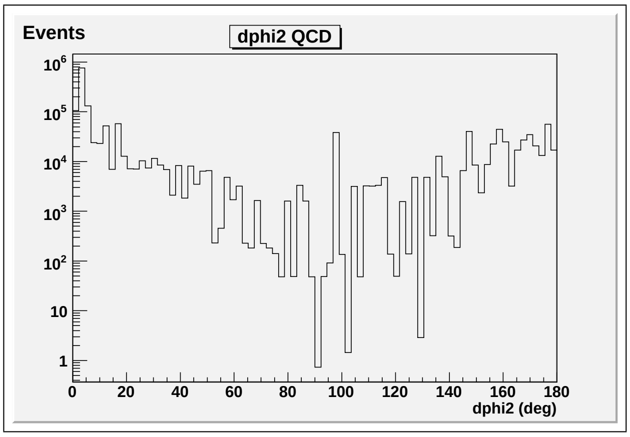

(a) QCD di-jet $\delta\phi_2$ plot

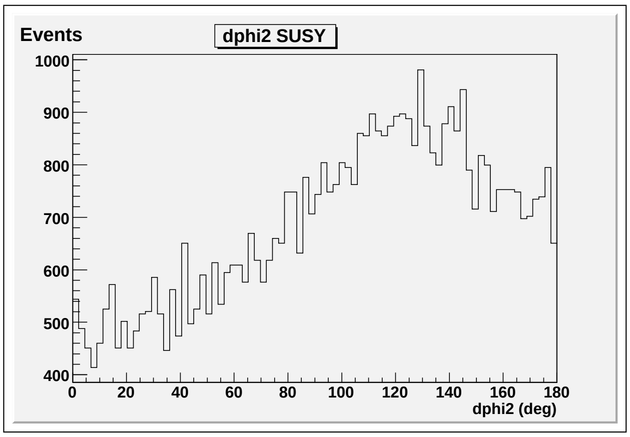

(b) SUSY $\delta\phi_2$ plot

Figure 4: $\delta\phi_2$ plots

The $\delta\phi$ plots in Figure 3 provide a pair of good discriminating cuts in the $\delta\phi_1$ – $\delta\phi_2$ plane. One can see that from these plots sensible cuts can be defined as in equations 5 and 6 that will help discriminate between QCD jets and SUSY.

$$R_1 = \sqrt{\delta\phi_2^2 + (\pi - \delta\phi_1)^2} \tag{5}$$

$$R_2 = \sqrt{\delta\phi_1^2 + (\pi - \delta\phi_2)^2} \tag{6}$$

For the purpose of this analysis cuts were made such that $R_1 > 0.5^c$ and $R_2 > 0.5^c$. This has the effect of cutting out the highly populated corner regions $(0,\pi)$ and $(\pi,0)$ in the $\delta\phi_1 - \delta\phi_2$ plane.

2.1.3 Transverse Sphericity S_T

Sphericity is the measure of the isotropy of the event in three-dimensional space. It is defined between 0 and 1 inclusive $0 \leq S \leq 1$, where 0 would correspond to a perfectly back-to-back event and 1 to a completely isotropic one. 'Transverse Sphericity' S_T, also known as circularity, is the extension of the same concept to the two-dimensional plane perpendicular to the beam axis.

The reason for considering this variable is that QCD di-jet events are expected to be back-to-back (i.e. $S_T = 0$); whereas, squark production events are not expected to be back-to-back due to their decay to other supersymmetric particles all along the SUSY decay chains, before the standard model jets are detected in the calorimeters.

The transverse sphericity is defined as in equation 7,

$$S_T = \frac{2\lambda_2}{(\lambda_1 + \lambda_2)} \tag{7}$$

where λ_1 and λ_2 are the eigenvalues of the 2×2 sphericity tensor $S_{ij} = \sum_k p_{ki}p^{kj}$.

This shows a sharp decrease with increasing sphericity for the QCD jet background as compared to the much slower decrease with the SUSY events. In accordance with the CMS TDR (5) the requirement of $S_T > 0.2$ was taken as the initial cut value to be optimised. Figure 5 however, would tend to suggest that a cut of $S_T > 0.1$ or even $S_T > 0.05$ would perform better at reducing the QCD jet background. For Figure 5 1000 events were processed for each J1-J8 sample and 7000 for the SU3 SUSY sample. The J1-J8 events were weighted and along with the SU3 SUSY sample events were normalised to unit area. The data sets and analysis code was as in section 2.1.1.

2.1.4 Effective Mass M_{eff}

Another variable considered was the so called 'effective mass' (M_{eff}), which is the scalar sum of the E_T^{Miss} and the p_T of the three hardest jets defined as in equation 8 below.

$$M_{eff} = E_T^{Miss} + p_{T,1} + p_{T,2} + p_{T,3} \tag{8}$$

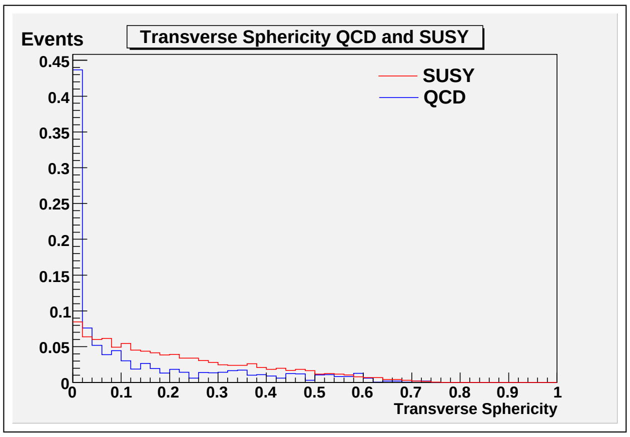

Figure 5: Transverse Sphericity Plot

It was expected that the SUSY squark production events would have higher M_{eff} than the QCD jet events owing to the higher E_T^{Miss}. The M_{eff} of both the QCD jet and SUSY events were plotted (Figure 6) for 7000 and 8000 events respectively and normalised to $10fb^{-1}$.

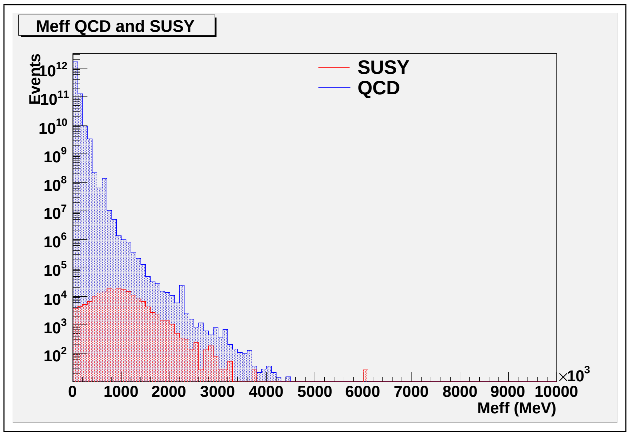

Figure 6: Meff Plot

The data sets and analysis code used were as in section 2.1.1. From these plots a requirement of $M_{eff} > 500$ GeV is suggested to help reduce the QCD background.

2.1.5 QCD Jet Removal

Having investigated these variables and proposed initial cut values, their efficacy in reducing the QCD jet background was to be tested. For this the M_{eff}

variable was again plotted for both QCD and SUSY only this time with all the cuts from the previous sections (jet cuts, E_T^{Miss} cuts, sphericity cuts and the $\delta\phi$ cuts) on, excluding of course the cut on the M_{eff} itself. The resultant plot can be seen in Figure 7.

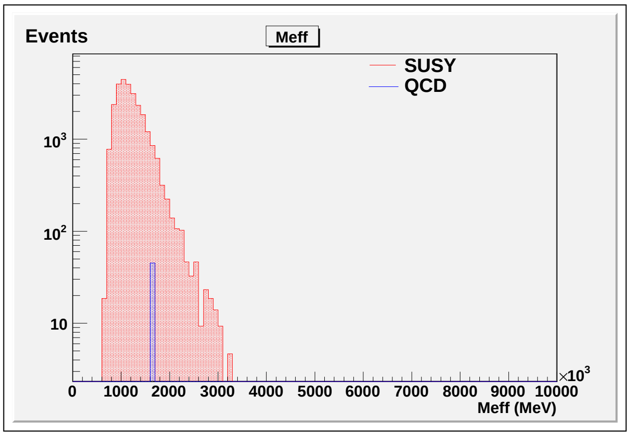

Figure 7: M_{eff} plot with cuts

From this plot the SUSY signal can clearly be seen to be higher than and distinguishable from that of the QCD jet background, the contribution from which having been significantly reduced.

The E_T^{Miss} distribution of both QCD and SUSY samples was also plotted with all cuts on except this time the cut on E_T^{Miss} itself. Here the resultant plot can be seen in Figure 8.

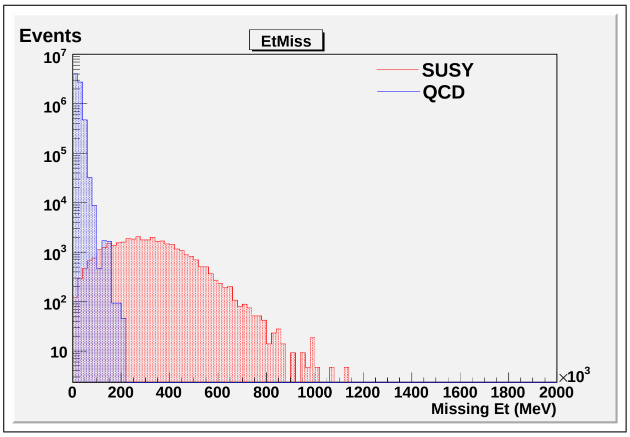

Figure 8: E_T^{Miss} plot with cuts

From this plot also the SUSY signal can clearly be seen to be greater than that of the QCD jets, above the cut value of $E_T^{Miss} > 200$ GeV.

The analysis for these plots was performed solely using the ATLAS offline software version 12.0.6, with data sets from the ATLAS production with the same version. With 10000 events processed per QCD J1-J8 sample and 40000 events processed for the SUSY squark production as in section 2.1.2. These plots have been normalised to $10fb^{-1}$.

2.1.6 W→ eν & Z→ $\nu\bar{\nu}$ Backgrounds

While the majority of this study so far has concentrated on optimising the reduction of the QCD jet background, there are several other SM processes that will contribute to a signature of jets and E_T^{miss}, namely production of W+Jets, Z+Jets events, $t\bar{t}$ pairs, di-bosons and single top. Of these, the W→ eν and Z→ $\nu\bar{\nu}$ have so far been looked at and are presented in this report.

After acquiring some background samples, namely W→ eν and Z→ $\nu\bar{\nu}$, the next task was to investigate how effective the variables and cuts already determined would be at reducing these additional backgrounds. To this end, the M_{eff} was re-plotted with all the aforementioned cuts; but this time, in addition to the SUSY and QCD jet events, the W→ eν events were also included. This yielded Figure 9.

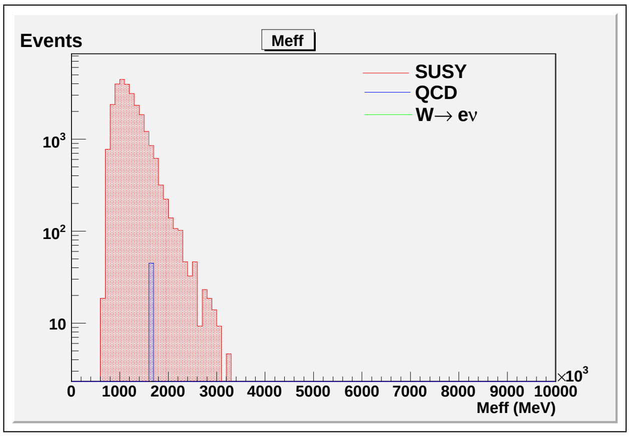

Figure 9: M_{eff} plot with W→ eν background added and with all cuts on

This shows that the combination of cuts applied in this analysis to reduce the QCD jet background also have the potential to provide some discriminating power between SUSY and W→ eν background as well.

Following this, the M_{eff} was again re-plotted with the W→ eν sample and all the relevant cuts just as before. This time however the Z→ $\nu\bar{\nu}$ event sample was also plotted on the same axis. This gave Figure 10.

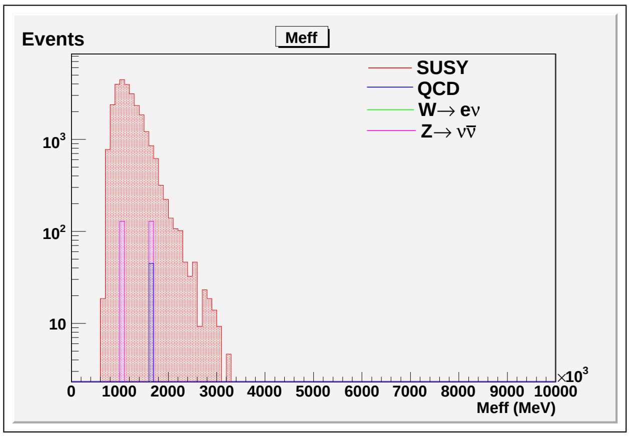

Figure 10: M_{eff} plot with both W→ eν and Z→ $\nu\bar{\nu}$ background samples added and with all cuts on

As can be seen, the cuts also reduce this Z→ $\nu\bar{\nu}$ background, though not by as much as that of the W→ eν it is still below the squark production curve.

For these plots, the ATLAS production 'JimmyWenu.recon' and 'pythia_Znunu_qg_Nj2.recon' samples, generated with release 12.0.6 were used. For the W→ eν data, 10000 events were processed, whilst for the Z→ $\nu\bar{\nu}$ data, 4500 events were processed. All analysis was performed using the ATLAS offline software release 12.0.6 and the plots were normalised to $10fb^{-1}$.

2.2 AtlFast Work

Since the ATLAS full chain simulation takes a long time it is often not practical to generate events in this manner. This led to the concept of the ATLAS fast simulation (AtlFast). AtlFast essentially takes the output from a generator and simply applies smearing functions to jump straight to the output AOD stage. It is however of great importance that in doing such a 'short cut' the physics is not in any way skewed, this explains the continuing effort to validate AtlFast.

As a natural continuation of (and of importance to) the work completed so far on jets and E_T^{Miss}, a comparison was carried out by request of the Atlfast group between the jet E_T and jet p_T spectra generated by Atlfast and that which was produced using the full chain simulated data.

Atlfast has its own inbuilt jet clustering algorithms which although sufficient for tasks in which jet finding is not a priority are by no means as sophisticated as those used in the full simulation, the so called JetRec algorithms. In the comparison therefore, the Atlfast data was passed through the JetRec algorithms as is the recommended way of working. In the plots below (Figure 11), the fast simulated data with no calibration represents JetRec created jets where the energy calibration has been switched off. For these plots, 10000 events were

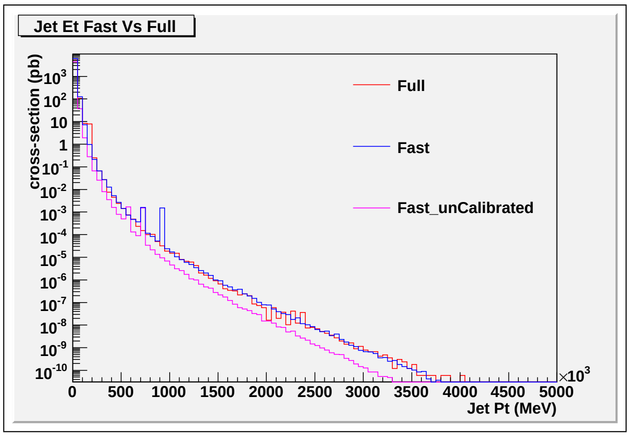

(a) Fast Vs Full Et Spectrum

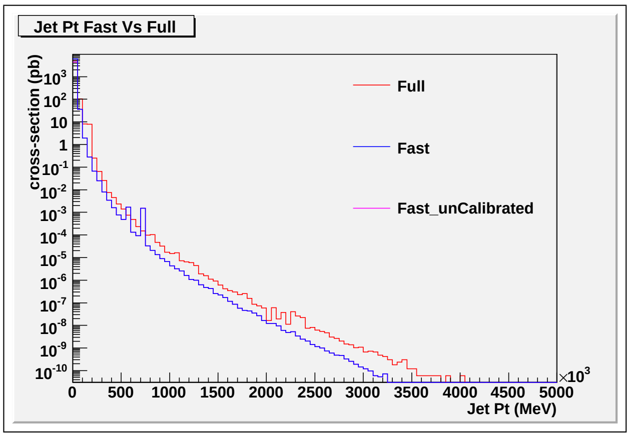

(b) Fast Vs Full Pt Spectrum

Figure 11: Fast Vs Full Simulation Plots

processed per J1-J8 sample for the AtlFast simulation data. The full simulation data were the ATLAS production 'pythia.jetjet.recon' J1-J8 samples from release 11.0.42 of which 1000 events were processed per J1-J8 sample. The fast simulation events were generated with AtlFast on the fly using the DC3 jobOptions with release 12.0.31. The JetRec algorithms for the AtlFast events were also implemented on the fly via a line in the DC3 jobOptions file. Both were Analysed using the ATLAS offline software version 12.0.31 and normalised to $10fb^{-1}$.

Of note is the lack in calibration of the p_T fast simulation plot. This was down to a computing oversight in which the calibration of p_T was left out and has been corrected in the most recent version.

2.3 SUSY CSC3 Note Work

The Computing System Commissioning (CSC) notes are physics groups studying specific physics processes using the official CSC full chain generated data sets.

The SUSY CSC3 group are looking at 'Data-driven Estimation of QCD Backgrounds to SUSY'. As this is directly related to the current jets and E_T^{Miss} analysis, and owing to the fact that some fast simulation versus full simulation investigations had already been performed, the transverse energy resolution was to be compared between the fast and full simulations. The plots (Figure 12)

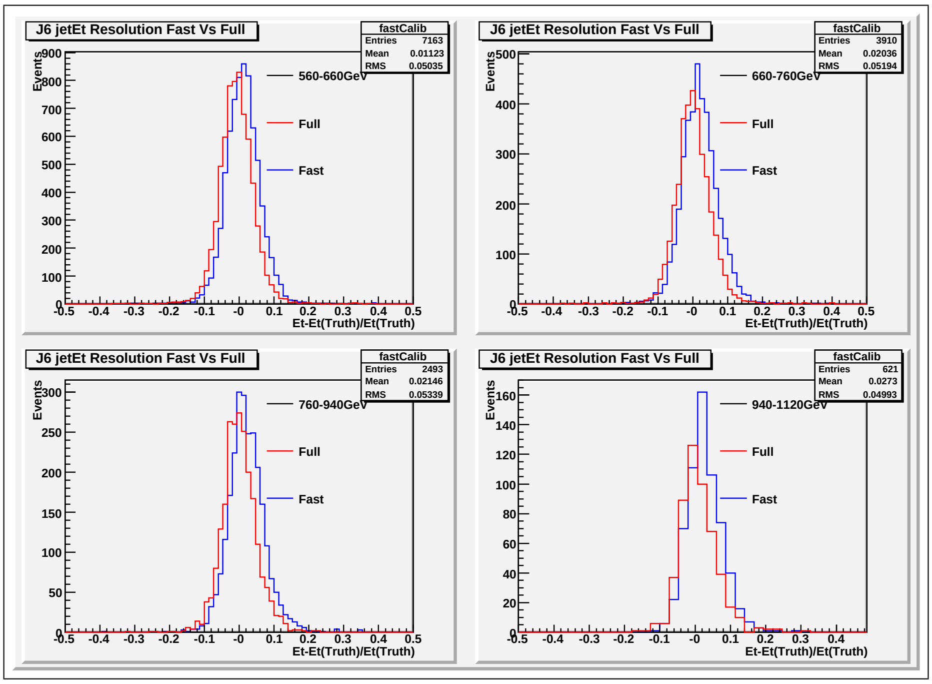

Figure 12: Energy resolution plots for the J6 sample, each plot is in a different p_T range

were produced using the same fast simulation samples as in section 2.2 above, with 10000 events per J1-J8 sample, while the full simulation samples were the ATLAS production 'pythia.jetjet.recon' J1-J8 samples using release 12.0.6 and both plots have been normalised to $10fb^{-1}$. The analysis was performed using the ATLAS offline software version 12.0.6.

In Figure 12 the difference between the fast and full simulations is quite noticeable even in the J6 sample where there was least difference. The true nature of these observed differences is still the subject of closer investigation as it was expected that there would be closer agreement between the two.

2.4 ATLAS RTT Framework

The Atlas 'Run Time Tester' Framework is designed as a tool for developers which provides them with a convenient way to test, on a nightly basis, both the status and the output that any changes to their code may have had. It allows one to automate:

- The running of Athena (as well as non-Athena) jobs.
- The running of post-job activities including ROOT macros, regression tests and user specified Python scripts.
- The publishing of all results to a user specified directory which can be web served for convenient retrieval anywhere.

In expectation of ultimately taking over the day to day looking after of both the 'Atlfast' and the 'Generators' package's RTT modules I have been familiarising myself with its workings, the main components of which being the 'unified configuration file' and the output log files.

[1] The fast simulation software for the ATLAS experiment see section 2.2

[2] ATLAS experiment physics group looking at 'Data-driven Estimation of QCD Backgrounds to SUSY' see section 2.3

[3] Official ATLAS production Pythia generated QCD jet samples in different p_T ranges, indicated by the J1-J8. Ranges: J1=17-35 GeV, J2=35-70 GeV, J3=70-140 GeV, J4=140-280 GeV, J5=280-560 GeV, J6=560-1120 GeV, J7=1120-2280 GeV, J8>2280 GeV

[4] Official ATLAS production Herwig/Jimmy generated SUSY SU3 bulk region sample. SUSY parameters: $m_0 = 100$ GeV, $m_{\frac{1}{2}} = 300$ GeV, $A_0 = -300$ GeV, $\tan\beta = 6$, $\mu > 0$

3 Future Study

As the analysis progresses, the need to study the full range of backgrounds will become important. In the near future the analysis will expand to include the backgrounds from $t\bar{t}$ events, both the hadronic and non-hadronic decay samples. The background for the Z→ee has also been obtained and will be included very soon. Following that, as many additional backgrounds as possible, including di-bosons and single top, will be added into the analysis.

Of note is that all of the samples considered in this report are generated with either Pythia or Herwig. These are not necessarily the most suitable and so in the future Alpgen Monte-Carlo samples will be studied. A trigger study will also be performed later on to look at optimising the trigger for these SUSY events.

Finally, when real data is available these studies can be applied to determine how well our Monte-Carlos are predicting both the 'standard model' and the 'beyond the standard model' physics and maybe to see some early signs of supersymmetry.

References

[1] Peter W. Higgs, *Broken Symmetries and the Masses of Gauge Bosons.* Physical Review Letters, Volume 13, Number 16, 19 October 1964.

[2] http://www.Wikipedia.org, *R-Parity.* 11 April 2007.

[3] ATLAS Collaboration, *ATLAS Detector and Physical Performance Technical Design Report.* Volume I, 1999.

[4] ATLAS Collaboration, http://atlas.ch/atlas_photos.html, *ATLAS Detector Photos.*

[5] CMS Collaboration, *CMS Physics, Technical Design Report.* Volume II, Physics Performance, 26 June 2006.